Acta Crystallographica Section A
**Foundations of Crystallography**
ISSN 0108-7673

Received 5 July 2004
Accepted 20 October 2004



# Short-range order and spin-glass-like freezing in *A*–Mg–*R* (*A* = Zn or Cd; *R* = rare-earth elements) magnetic quasicrystals

**Taku J. Sato**

Neutron Science Laboratory, Institute for Solid State Physics, University of Tokyo, 106-1 Shirakata, Tokai, Ibaraki 319-1106, Japan, and SORST, Japan Science and Technology Agency, Kawaguchi, Saitama 332-0012, Japan. Correspondence e-mail: taku@issp.u-tokyo.ac.jp

Recent progress in experimental understanding of the *A*–Mg–*R* (*A* = Zn and Mg, *R* = rare-earth elements) magnetic quasicrystals is reviewed. The *A*–Mg–*R* quasicrystals have long been classified as spin-glasses because of their typical spin-freezing behavior at low temperatures. On the other hand, recent neutron diffraction experiments clearly detect strong magnetic diffuse scattering, indicative of significant short-range spin order. After all the data sets obtained by various experimental techniques have been combined, it is proposed that the nature of the spin freezing in magnetic quasicrystals is related to blocking phenomena in superparamagnets rather than to a thermodynamic transition in the canonical spin-glasses.

## 1. Introduction

Quasicrystals are characterized by sharp Bragg reflections with a point symmetry that is forbidden in a periodic lattice, such as the fivefold symmetry. The appearance of Bragg reflections evidently demonstrates highly ordered atomic structure, nevertheless, the forbidden point symmetry indicates absence of periodicity in the underlying lattice. These seemingly inconsistent characteristics of quasicrystals evoke a new category of atomic structure in solids, called *quasiperiodic* structure. Today, it is widely accepted that the atomic structure of the icosahedral quasicrystals is given as a projection of a six-dimensional (6D) hypercubic crystal into the three-dimensional (3D) physical space (Yamamoto, 1996; Steurer & Haibach, 1999). The *slope* of the 3D space relative to the 6D space is irrational (or more precisely, it is given by the golden ratio $\tau$), and thus the resulting atom arrangement in the 3D space becomes aperiodic. The aperiodic structure, nevertheless, gives rise to sharp Bragg reflections, owing to its hidden periodicity inherited from the original periodic lattice in the 6D space.

The quasicrystal was first discovered in a splat-cooled Al–Mn alloy (Shechtman *et al.*, 1984). Since then, a number of quasicrystalline phases have been discovered in various kinds of alloy systems (Tsai, 1999). Among them, an outstanding finding is the thermodynamically stable quasicrystals, exemplified by Al–Li–Cu–Mg (Ball & Lloyd, 1985), Al–Cu–Fe (Tsai *et al.*, 1987) and Ga–Mg–Zn (Ohashi & Spaepen, 1987) quasicrystals, and the following success of the single-grain growths (Tsai *et al.*, 1999). High-quality single-grained quasicrystals enable us to perform a detailed study on their structures. For example, high-quality single grains of Al–Pd–Mn and Al–Ni–Co quasicrystals accelerate atomic structure determination by means of the single-crystal X-ray diffraction technique (Boudard & de Boissieu, 1999; Cervellino *et al.*, 2002; Yamamoto *et al.*, 2003).

On the other hand, it has always been an attractive issue to find anomalous physical properties originating from quasiperiodicity. Since quasiperiodicity is, in its basic concept, defined in the long-length-scale limit, such an anomaly was believed to appear in the physics of spatially spread states, such as electron and phonon wavefunctions. Thus, continuous efforts have been devoted to finding such anomalies in thermal and electric transports, electron density of states and atomic vibrations (Hafner & Krajčí, 1999). A theoretical study on these lines indeed shows anomalous behavior, such as 'spiky peaks and pseudo gap at the Fermi level in the electronic density of states' (Fujiwara, 1989; Fujiwara & Yokokawa, 1991), or 'criticality in electron wavefunctions in low-dimensional quasicrystals' (Tsunetsugu *et al.*, 1986; Kohmoto *et al.*, 1987; Fujiwara, 1989; Hiramoto & Kohmoto, 1989; Tsunetsugu *et al.*, 1991). Nevertheless, those anomalies in real quasicrystals have been a controversial issue on the experimental side.

The magnetic order of localized moments (spins) in quasiperiodic structures has also been a fundamental issue of study. Theoretically, non-trivial magnetic ordering has been suggested for spin systems in ideal quasiperiodic structures (Achiam *et al.*, 1986; Godrèche *et al.*, 1986; Tsunetsugu & Ueda, 1987; Aoyama & Odagaki, 1987; Okabe & Niizeki, 1990; Ledue *et al.*, 1993; Reid *et al.*, 1998; Lifshitz, 1998). On the other hand, experimental studies have long been restricted to the aluminium–transition-metal quasicrystals, which were the only *magnetic* quasicrystals (Matsuo *et al.*, 1993; Chernikov

*et al.*, 1993; Bahadur, 1997) until 1993. In these quasicrystals, the magnetic moments cannot be regarded as localized, since they originate from the itinerant *d* electrons of the transition metals. The formation of magnetic moment itself is very sensitive to the local environment, which substantially complicates the analysis of the magnetic properties (Rau *et al.*, 2003). Thus, it is not straightforward to elucidate the intrinsic nature of spin order in quasiperiodic structures from the experimental results.

In the last decade, several types of icosahedral quasicrystals have been discovered in the *A*–Mg–*R* system with *A* = Zn or Cd and *R* = rare-earth elements (Luo *et al.*, 1993; Niikura *et al.*, 1994; Tsai *et al.*, 1994; Guo *et al.*, 2000; Sterzel *et al.*, 2002). These quasicrystals are unique since they have well localized and sizable 4*f* magnetic moments of the rare-earth elements in the quasiperiodic lattice, and thus provide an opportunity to study the ordering of localized spins in the quasiperiodic structure. Because of this advantage, the *A*–Mg–*R* icosahedral quasicrystals have been intensively studied using various experimental techniques. The primary purpose of this review is to give a comprehensive summary of the magnetic properties of the *A*–Mg–*R* quasicrystals. A survey is presented on the macroscopic magnetic properties, such as magnetization, as well as on microscopic information obtained by neutron diffraction and muon spin resonance (μSR). After combining all the existing data sets, we discuss the ordering of the localized spins in the quasiperiodic lattice, and try to elucidate our present understanding and remaining questions on this issue.

The rest of the paper is organized as follows. In the next section, information on atomic structure will be presented. §3 is devoted to the magnetization measurements. Neutron diffraction results are summarized in §4, together with a simple model spin configuration in the short-range-ordered regions. §5 gives a summary of dynamical aspects of quasicrystalline magnets. In §6, our present understanding on spin ordering is addressed, and conclusions follow. A complementary review on earlier bulk magnetic studies can be found in the literature (Fukamichi, 1999).

## 2. *A*–Mg–*R* quasicrystals and their structures

Three different types of rare-earth-based magnetic quasicrystals have been reported to date: (I) face-centered icosahedral Zn–Mg–*R* quasicrystals (*f*-Zn–Mg–*R*); (II) primitive icosahedral Zn–Mg–*R* quasicrystals (*p*-Zn–Mg–*R*); (III) primitive icosahedral Cd–Mg–*R* quasicrystals (*p*-Cd–Mg–*R*). Historically, the first discovery was the icosahedral phase in the Zn–Mg–Y alloy, of which the lattice type was unidentified (Luo *et al.*, 1993). This work was followed by Niikura *et al.* (1994) and Tsai *et al.* (1994), who demonstrated that the quasicrystalline phase in an alloy with composition $Zn_{50}Mg_{42}R_8$ is indeed face-centered icosahedral, thermodynamically stable, and forms for several different rare-earth elements (*R* = Gd, Tb, Dy, Ho, Er and Y). Because of its thermodynamical stability and single-grain availability, the structure of the *f*-Zn–Mg–*R* quasicrystals has been extensively studied by a number of methods, including single-crystal X-ray diffraction (Takakura *et al.*, 2001), high-resolution electron microscopy (Abe *et al.*, 2001), extended X-ray absorption fine-structure (EXAFS) measurements (Charrier *et al.*, 1998) and pair-distribution-function (PDF) analysis (Brühne *et al.*, 2003). As a result, the atomic structure of the *f*-Zn–Mg–*R* quasicrystals is largely determined, at least for the rare-earth sites. (They can be rather easily determined due to their large X-ray and electron scattering amplitudes.) By applying the low-density elimination method to the single-crystal X-ray diffraction data, Takakura *et al.* (2001) showed that the occupation domains of the rare-earth elements are at $(\frac{3}{4}, \frac{1}{4}, \frac{1}{4}, \frac{1}{4}, \frac{1}{4}, \frac{1}{4})$ in the 6D hypercubic lattice. A synchrotron-radiation X-ray powder diffraction study by Ishimasa *et al.* (2003) also gives a consistent result; it further infers a size of the occupation domain as $r = 7.419\,(3)$ Å in a spherical approximation. To see the characteristics of the rare-earth-site network, we have generated the rare-earth sites in a spherical region of $r < 100$ Å around the origin, using the parameters

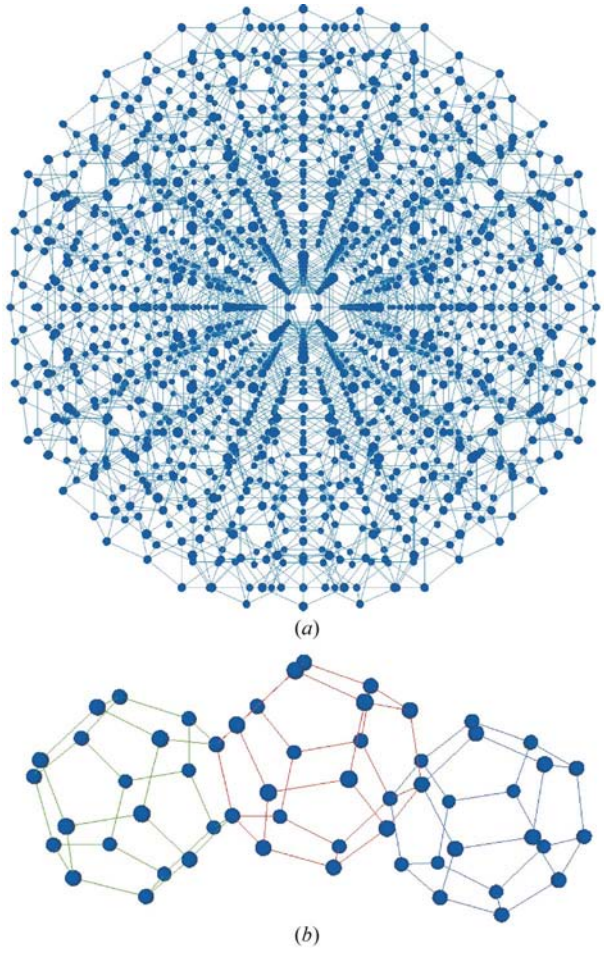


**Figure 1**
(*a*) Rare-earth sites ($r < 40$ Å around the origin) in the *f*-Zn–Mg–*R* icosahedral quasicrystals generated using the parameters determined by the synchrotron-radiation powder X-ray experiment (Ishimasa *et al.*, 2003). (*b*) Magnified illustration of the edge-sharing dodecahedral network of the rare-earth sites; only atoms participating in the network are shown.

given above. Shown in Fig. 1(*a*) is part of the generated rare-earth sites ($r < 40$ Å). We have found that the skeleton of the atomic structure is described by a network of edge-sharing dodecahedra of which the edge length is 5.5 Å. Fig. 1(*b*) is a magnified figure showing part of the network consisting of three dodecahedra. By analyzing the generated structure, we found that approximately 66% of the rare-earth sites participate in the dodecahedron network. It should be noted that generally spherically approximated occupation domains tend to give a considerable number of missing and extra atoms in the projected structure. We thus suggest that the appearance of the remaining (non-participating) atoms may be due to the spherical approximation used in the structure determination; they may not intrinsically exist in the real quasicrystal. Further structural analysis using more elaborate polygonal occupation domains is highly desirable.

The *p*-Cd–Mg–*R* quasicrystals were found in 2000 by Guo *et al.* (2000), in relation to the discovery of the epoch-making binary Cd–Yb quasicrystal (Tsai *et al.*, 2000). Because of their rather recent discovery, the structural study has not yet been completed. The *p*-Zn–Mg–*R* quasicrystals were found in 2002 by Sterzel *et al.* (2002). Only the 3D local atomic structure of the *p*-Zn–Mg–*R* quasicrystals has been inferred from the PDF analysis by Brühne *et al.* (2004); a structure determination using 6D crystallography has not been reported to date.

## 3. Macroscopic properties of the *A*–Mg–*R* quasicrystals

### 3.1. *f*-Zn–Mg–*R* quasicrystals

Since the first report by Hattori, Niikura *et al.* (1995), the magnetic susceptibility of the *f*-Zn–Mg–*R* icosahedral quasicrystals has been measured by several groups (Hattori, Niikura *et al.*, 1995; Charrier & Schmitt, 1997, 1998; Fisher *et al.*, 1999; Kashimoto *et al.*, 1999; Dolinšek *et al.*, 2001). Shown in Fig. 2 is the inverse susceptibility of the *f*-Zn–Mg–*R* quasicrystals for *R* = Tb, Dy, Ho and Er (Fisher *et al.*, 1999). The inverse susceptibility obeys the Curie–Weiss law at high temperatures:

$$\frac{1}{\chi} = \frac{3k_{\rm B}(T-\Theta)}{N_{\rm A}\mu_{\rm eff}^2}, \qquad (1)$$

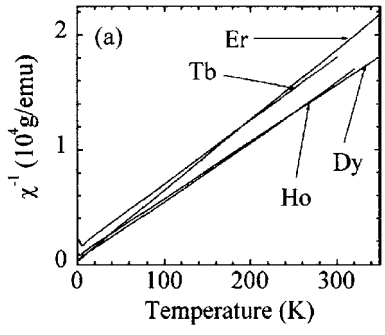


**Figure 2**
Inverse susceptibility of the *f*-Zn–Mg–*R* (*R* = Tb, Dy, Ho and Er) quasicrystals in the high-temperature region. Reprinted figure with permission from Fischer *et al.* (1999). *Phys. Rev. B*, **59**, 308–321. Copyright (1999) by the American Physical Society.

**Table 1**
Summary of magnetic parameters obtained for the *f*-Zn–Mg–*R* (Fisher *et al.*, 1999) and *p*-Cd–Mg–*R* (Sato, Guo & Tsai, 2001) quasicrystals.

$\mu_{\rm eff}$, $\mu_{R^{3+}}$, $\Theta$, $T_{\rm f1}$ and $T_{\rm f2}$ are the effective moment, calculated moment for free $R^{3+}$ ions, Weiss temperature, upper freezing temperature and lower freezing temperature (if it exists).

| System | $\mu_{\rm eff}$ ($\mu_{\rm B}$) | $\mu_{R^{3+}}$ ($\mu_{\rm B}$) | $\Theta$ (K) | $T_{\rm f1}$ (K) | $T_{\rm f2}$ (K) |
|---|---|---|---|---|---|
| Zn–Mg–Tb | 9.91 | 9.72 | −26.3 | 5.80 | – |
| Zn–Mg–Dy | 10.5 | 10.63 | −14.8 | 3.60 | – |
| Zn–Mg–Ho | 10.4 | 10.60 | −7.8 | 1.95 | – |
| Zn–Mg–Er | 9.49 | 9.59 | −5.1 | 1.30 | – |
| Cd–Mg–Gd | 7.90 | 7.94 | −37 | 13.0 | 4.8 |
| Cd–Mg–Tb | 10.03 | 9.72 | −23 | 12.5 | 5.6 |
| Cd–Mg–Dy | 10.67 | 10.63 | −14 | 7.4 | 3.8 |
| Cd–Mg–Ho | 10.42 | 10.60 | −7 | 12.5 | 5.0 |
| Cd–Mg–Er | 9.71 | 9.59 | −6 | 4.4 | – |
| Cd–Mg–Tm | 7.08 | 7.57 | −2 | – | – |

where $k_{\rm B}$, $\Theta$, $N_{\rm A}$ and $\mu_{\rm eff}$ are the Boltzmann factor, Weiss temperature, Avogadro number and effective moment, respectively. These parameters, obtained by the Curie–Weiss law fitted to the data above 50 K, are listed in Table 1. [To convert the Curie constants *C* given in the original report by Fisher *et al.* (1999) to $\mu_{\rm eff}$, we assume the chemical composition of the Zn–Mg–*R* quasicrystals to be $Zn_{56.8}Mg_{34.6}R_{8.7}$.] These effective moments are almost equal to those of the $R^{3+}$ free ions, indicating that the magnetic moments of the rare-

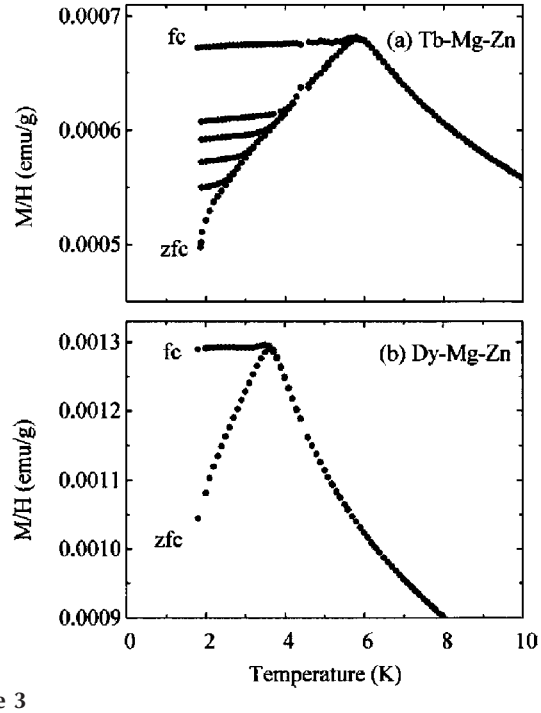


**Figure 3**
(*a*) Temperature dependence of the magnetization divided by the external field for the *f*-Zn-Mg-Tb quasicrystal. Results for the zero-field cooling (zfc), field cooling (fc) and several intermediate-condition runs are shown. (*b*) Results for the *f*-Zn-Mg-Dy quasicrystal; the zero-field cooling (zfc) and field cooling (fc) runs are shown. See the original work for details. Reprinted figure with permission from Fischer *et al.* (1999). *Phys. Rev. B*, **59**, 308–321. Copyright (1999) by the American Physical Society.

earth elements are well localized with no significant crystalline-electric field (CEF) splitting.

Shown in Figs. 3(*a*) and 3(*b*) are the temperature dependence of the magnetization at low temperatures for $R$ = Tb and Dy (Fisher *et al.*, 1999). Cusp-like anomalies clearly appear in the zero-field-cooled magnetization at $T$ = 5.8 and 3.6 K for Tb and Dy, respectively. Below the anomaly temperatures, large irreversibility for the zero-field-cooled and field-cooled magnetizations is observed. This magnetization behavior is very similar to that of the canonical spin-glasses, such as the Cu–Mn alloy, where the anomaly is interpreted as a thermodynamic transition into a randomly frozen spin state (Binder & Young, 1986; Mydosh, 1993). The other rare-earth systems behave quite similarly except for the difference in temperature scales, and thus the earlier magnetization studies concluded that the *f*-Zn–Mg–*R* quasicrystals fall into the same class as the canonical spin-glasses.

### 3.2. *p*-Cd–Mg–*R* quasicrystals

The bulk magnetization of the *p*-Cd–Mg–*R* quasicrystals has been studied in detail by Sato, Guo & Tsai (2001) and Sebastian *et al.* (2004). At high temperatures, magnetization of the *p*-Cd–Mg–*R* quasicrystals is mostly identical to that of the *f*-Zn–Mg–*R* quasicrystals. Shown in Figs. 4(*a*) and 4(*b*) are the magnetic susceptibility and inverse susceptibility of the *p*-Cd–Mg–*R* quasicrystals. Except for the non-magnetic *p*-Cd–Mg–Yb quasicrystal, Curie–Weiss-type paramagnetic increase was clearly seen in the susceptibility as temperature is decreased. The effective moments, estimated by the Curie–Weiss fit [equation (1)], are listed in Table 1; they are in good agreement with the calculated values for the free $R^{3+}$ ions. At low temperatures, two anomalies appear in the dc magnetization, in contrast to the single freezing behavior in the *f*-Zn–Mg–*R*

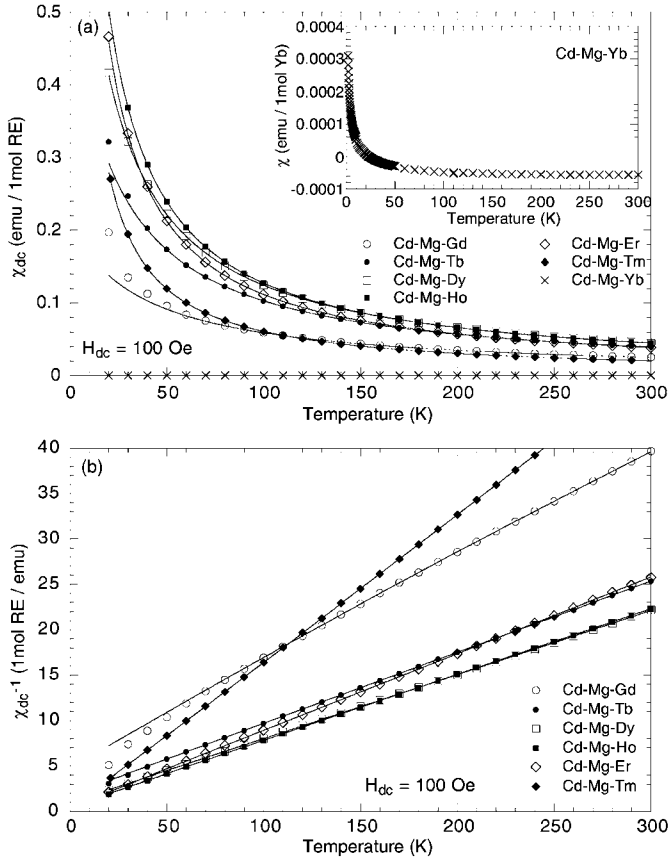


**Figure 4**
(*a*) Dc magnetic susceptibility of the *p*-Cd–Mg–*R* (*R* = Gd, Tb, Dy, Ho, Er, Tm and Yb) quasicrystals in the high-temperature region. Inset: magnified plot for the *p*-Cd–Mg–Yb quasicrystal; note that the susceptibility is three orders of magnitude smaller than the others, indicating that Yb is exceptionally in the non-magnetic $Yb^{2+}$ state. (*b*) Inverse susceptibility of the *p*-Cd–Mg–*R* (*R* = Gd, Tb, Dy, Ho, Er and Tm) quasicrystals. Reprinted with permission from Sato, Guo & Tsai (2001). *J. Phys. Condens. Matter*, **13**, L103–L111. Copyright (2001) Institute of Physics Publishing.

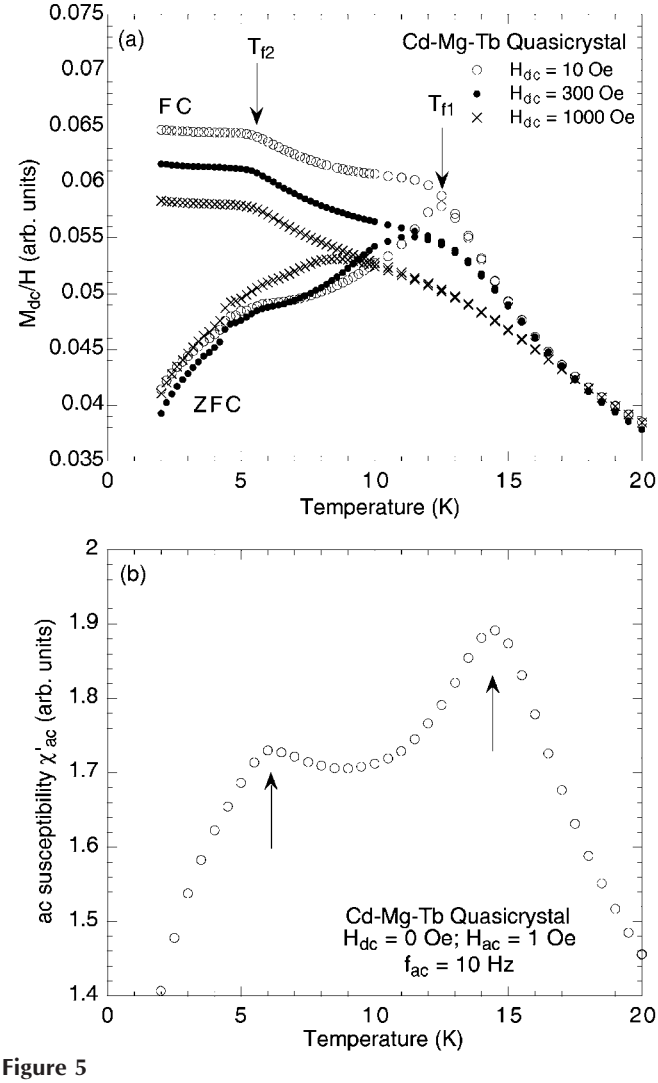


**Figure 5**
(*a*) Temperature dependence of the dc magnetization divided by the external field for the *p*-Cd–Mg–Tb quasicrystal; the zero-field cooling (ZFC) and field cooling (FC) runs, measured under several external magnetic fields, are shown. (*b*) Temperature dependence of the real part of the ac susceptibility. Reprinted with permission from Sato, Guo & Tsai (2001). *J. Phys. Condens. Matter*, **13**, L103–L111. Copyright (2001) Institute of Physics Publishing.

quasicrystals (Sato, Guo & Tsai, 2001); representative data obtained for *p*-Cd–Mg–Tb quasicrystal are shown in Fig. 5(*a*). The ac susceptibility clearly detects the two anomalies, as shown in Fig. 5(*b*). In view of the field irreversibility accompanying the anomalies, it is speculated that both of them are indicative of spin freezing. While the polycrystalline experiments detect two successive anomalies, in the recent single-grain experiments for selected $R$ = Gd, Tb and Dy by Sebastian *et al.* (2004), the freezing appears as a rather broad but single peak in the zero-field-cooled magnetization (except for Gd), being indicative of several (distributed) freezing temperatures. Therefore, it may be plausible that the freezing behavior is strongly affected by the sample quality, with an intrinsic tendency to have a distribution in freezing temperatures. Conclusive microscopic interpretation of the spin freezing in *p*-Cd–Mg–*R* is, thus, hardly obtained solely from the magnetization data.

### 3.3. *p*-Zn–Mg–*R* quasicrystals

A magnetic study on this class of quasicrystals is highly desired since it may reveal the effect of the lattice-type difference on the magnetism; a direct comparison between the primitive icosahedral and face-centered icosahedral lattices becomes possible in the same alloy system using the *p*-Zn–Mg–*R* and *f*-Zn–Mg–*R* quasicrystals. Experiments along this line are now in progress.

## 4. Microscopic spin correlations

The knowledge we can obtain from the macroscopic magnetization measurements is limited, and thus it is hardly conclusive whether the anomaly observed in the magnetization is really a sign of the canonical spin-glass transition or not. Neutron diffraction is a unique technique that provides indispensable microscopic information on spin ordering. Hence, several neutron diffraction studies have been carried out on the *A*–Mg–*R* magnetic quasicrystals to date.

### 4.1. Powder neutron diffraction on the *f*-Zn–Mg–*R* quasicrystals

Pioneering work in this field is the powder neutron diffraction of the *f*-Zn–Mg–*R* quasicrystals by Charrier *et al.* (1997). They reported coexisting magnetic Bragg reflections and diffuse scattering, both of which simultaneously develop below $T_N$, where $T_N \simeq 20, 12, 7$ and 5 K for the Tb, Dy, Ho and Er systems, respectively. They claimed that the Bragg reflections can be indexed by quasiperiodic indices with the 6D magnetic modulation vector $\mathbf{q}_m = (\frac{1}{4}, 0, 0, 0, 0, 0)$ (using the original definition of the 6D lattice by Charrier *et al.* (1997). From this result, they concluded that quasiperiodic magnetic long-range order is established below $T_N$. The order is suggested to be *antiferromagnetic* in the 6D space.

This magnetic long-range order was, however, questioned by other experiments. In the magnetic susceptibility and specific heat measurements, it was impossible to see any anomaly at the transition temperature $T_N$ (Hattori, Fukamichi *et al.*, 1995; Hattori, Niikura *et al.*, 1995; Charrier & Schmitt, 1997, 1998). The μSR measurements also exhibit no spontaneous spin precession even at the lowest temperature (Noakes *et al.*, 1998; Charrier *et al.*, 1999). Crucial information on this puzzle was obtained in two neutron diffraction studies with high-quality samples. One is by Islam *et al.* (1998), who use powdered single grains as a sample, which, in principle, contains only the quasicrystalline phase. They have observed only the magnetic diffuse scattering part of the preceding study even at the lowest temperature, and concluded that the magnetic long-range order is *not* robust in the quasicrystals. The other is by Sato *et al.* (Sato, Takakura, Tsai & Shibata, 1998; Sato *et al.*, 2000), who performed both powder and single-quasicrystalline neutron diffraction. They first carried out a metallographic survey for this Zn–Mg–*R* alloy system. Shown in Fig. 6 is the back-scattered electron micrograph of the polycrystalline $Zn_{50}Mg_{42}Ho_8$ sample prepared under conditions identical to the preceding experiment of Charrier *et al.* (1999). One may find several coexisting phases in addition to the icosahedral quasicrystalline phase (labeled *i*-QC). One of them was the magnetic $(Zn, Mg)_5Ho$ crystalline phase, and thus the neutron diffraction data from this sample are inevitably contaminated by magnetic scattering from the crystalline phase. They then obtained both the magnetic phases, *i.e.* the quasicrystalline and crystalline phases, in a single-phase form by tuning the sample-preparation conditions, and performed the neutron diffraction experiment for each phase. Shown in Fig. 7(*a*) is the diffraction pattern recorded at $T$ = 20 K, used as a paramagnetic reference, as well as the intensity difference between the lowest and the paramagnetic temperatures $[I(T = 1.6\ \text{K}) - I(T = 20\ \text{K})]$, regarded as an estimate of the magnetic scattering at the lower temperature. It is clear that the single-phase quasicrystalline sample shows only the diffuse scattering part. On the other hand, the magnetic signal $[I(T = 1.5\ \text{K}) - I(T = 20\ \text{K})]$ from the $(Zn, Mg)_5Ho$ phase (Fig. 7*b*) consists of Bragg reflections appearing at the same positions as

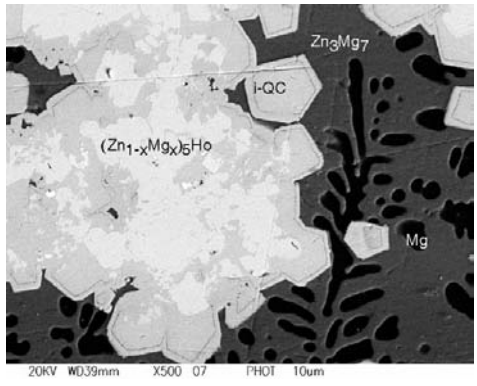


**Figure 6**
Back-scattered electron micrograph of the $Zn_{50}Mg_{42}Ho_8$ alloy, prepared under the same conditions as in Charrier *et al.* (1997); the as-cast alloy was annealed at 873 K for 20 min and subsequently at 673 K for 48 h. A magnetic crystalline phase remains with a composition of $(Zn_{1-x}Mg_x)_5Ho$ ($x \sim 0.2$), in addition to the quasicrystalline phase ($Zn_{57}Mg_{33}Ho_{10}$; *i*-QC). Reprinted figure with permission from Sato *et al.* (1998). *Phys. Rev. Lett.* **81**, 2364–2367. Copyright (1998) by the American Physical Society.

in the preceding report (Charrier *et al.*, 1997). It is thus concluded that the intrinsic spin order in the magnetic quasicrystal is only *short ranged*; the long-range order in the first report should be attributed to the crystalline phase.

### 4.2. Powder neutron diffraction on the *p*-Cd–Mg–*R* quasicrystals

A neutron powder diffraction study on the p-Cd–Mg–*R* quasicrystals has been performed by Sato *et al.* (2002). The neutron diffraction is generally difficult for the Cd-based compounds because of the strong thermal-neutron absorption of $^{113}$Cd, which has a natural abundance of about 12%. They thus used the isotope-enriched $^{114}$Cd to reduce the absorption. The powder neutron diffraction patterns were taken at $T = 2.5$, 10, and 30 K using the *p*-$^{114}$Cd–Mg–Tb quasicrystal. The higher-temperature data ($T$ = 30 K), shown in Fig. 8(*a*), were assumed to be a paramagnetic reference, and were subtracted from the two low-temperature data sets to see the development of magnetic scattering at the low temperatures. Figs. 8(*b*) and 8(*c*) show the estimated magnetic scattering intensity at the two low temperatures ($T$ = 2.5 or 10 K). The magnetic scattering consists of broad diffuse scattering peaks; absence of sharp Bragg reflections confirms the short-range nature of the spin ordering in the *p*-Cd–Mg–*R* quasicrystals. It should be remembered that there are two freezing temperatures in the polycrystalline sample of the *p*-Cd–Mg–Tb quasicrystals at $T_{f1}$ = 12.5 K and $T_{f2}$ = 5.6 K (Table 1). Nonetheless, one does not see any qualitative change in the diffuse scattering patterns at $T$ = 2.5 and 10 K. From this result, they conclude that the short-range order is essentially the same for the intermediate- and low-temperature phases, and that the freezing at $T_{f2}$ may have a slower time scale that cannot be identified by neutron scattering. This may also be consistent with the broadened freezing behavior indicated from the single-grain experiments (Sebastian *et al.*, 2004). The nature of the second freezing point (or distribution of freezing temperatures) may possibly be investigated by techniques sensitive for slower dynamics, such as the ac susceptibility and μSR measurement.

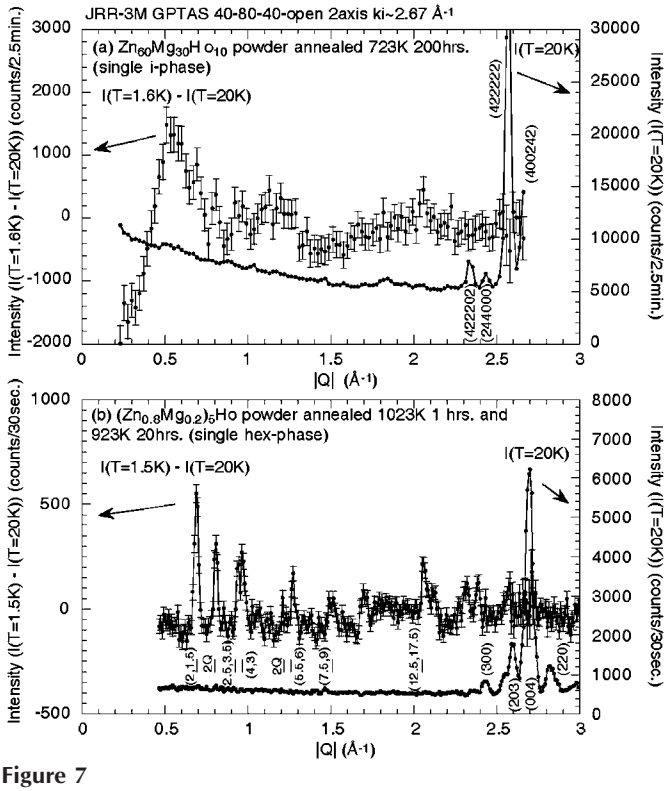


**Figure 7**
(*a*) Powder neutron diffraction pattern from the single-phased *f*-Zn–Mg–Ho quasicrystalline sample obtained by annealing the as-cast $Zn_{60}Mg_{30}Ho_{10}$ alloy for 200 h at 723 K. The magnetic contribution was estimated by subtracting higher-temperature (20 K) data from low temperature (1.5 K) data. (*b*) Powder neutron diffraction pattern for the $(Zn_{1-x}Mg_x)_5Ho$ crystalline phase at $T$ = 20 K, as well as the difference $I(T = 1.5\ \text{K}) - I(T = 20\ \text{K})$. The Bragg reflections are intentionally indexed by the quasicrystalline (irrational) indices (Charrier *et al.*, 1997), however, it has to be remembered that the Bragg reflections are from a crystalline phase; quasicrystalline indices exist densely in 3D $Q$ space, and thus any $Q$ point can be indexed if one uses indices with large perpendicular components. Reprinted figure with permission from Sato *et al.* (1998). *Phys. Rev. Lett.* **81**, 2364–2367. Copyright (1998) by the American Physical Society.

### 4.3. Single quasicrystal neutron diffraction on the *f*-Zn–Mg–*R* quasicrystals

The powder neutron diffraction experiments reveal that long-range magnetic order is absent in the *f*-Zn–Mg–*R* and *p*-Cd–Mg–*R* magnetic quasicrystals, and the intrinsic magnetic order is only of short range even at the lowest temperature. As is well known, the powder diffraction experiments give only the spherical average of the magnetic scattering in the reciprocal-lattice space, so that one cannot obtain the **Q**-directional dependence, which is indispensable information to elucidate details of spin correlations. Single-quasicrystal neutron diffraction experiments have been carried out by Sato, Takakura & Tsai (1998). They selected the *f*-Zn–Mg–Ho quasicrystal, of which the single-grain growth is relatively easy.

Overall features of the diffuse scattering were first investigated by measuring the scattering intensity in the planes with twofold, threefold and fivefold symmetry (2f, 3f and 5f) at the two temperatures; the lowest temperature $T \simeq 1.3$ K and the paramagnetic temperature $T$ = 20 K. Then, the magnetic scattering was deduced by the difference $I(T = 1.3\ \text{K}) - I(T = 20\ \text{K})$. This procedure was further justified by polarized neutron experiments (Sato *et al.*, 2000). The magnetic scattering was measured in a doubled symmetrically independent region in each plane, which is shown in Fig. 9 by solid yellow lines. After confirming that the magnetic scattering in the two independent regions is identical, the scattering data were folded into a single independent region to increase the statistical precision, and then they were unfolded to the full circle to improve the visibility of the symmetric features.

The resulting magnetic scattering intensity maps are shown in Figs. 9(*a*), 9(*b*) and 9(*c*) for the 2f, 3f and 5f planes, respectively. Positions of the intense nuclear Bragg reflections are also shown by blue dots in the first quadrant of Fig. 9. Apparently, the magnetic scattering is not spherical but is highly structured with a number of spot-like peaks, connected

by weak diffuse-scattering ridges. By comparing them with the nuclear Bragg positions, one can easily see that the diffuse scattering appears around the intense nuclear Bragg reflections. Thus, the short-range spin correlations are dominantly antiferromagnetic, which was first suggested from the magnetic susceptibility (Hattori, Niikura *et al.*, 1995). The spot-like peaks were examined in detail by performing several **Q** scans. As representative scans, the peak profiles around $\mathbf{Q} = (0, 0.55, 0)$ Å$^{-1}$ along the $Q_x$ and $Q_y$ directions are shown in Figs. 10(*a*) and 10(*b*), respectively. They obviously have finite widths, confirming the diffuse scattering nature of the seemingly spot-like peaks. The peak widths give an estimate of the correlation lengths of about $\xi \sim 10$ Å in half-width at half-maximum (HWHM). Shown in Fig. 10(*c*) is the temperature dependence of the peak intensity at $\mathbf{Q} = (0.55, 0, 0)$ Å$^{-1}$. The intensity increases below $T_{\rm SRC} \simeq 5$ K, indicating that the spin correlations develop below this temperature. This almost corresponds to the beginning of the deviation of the susceptibility from the Curie–Weiss law (Kashimoto *et al.*, 1999). We note that $T_{\rm SRC}$ is considerably higher than $T_{\rm f} = 1.95$ K. Hence, the spin correlations in $T_{\rm f} < T < T_{\rm SRC}$ are dynamic. The dynamic spin correlations can be observed so long as the spin

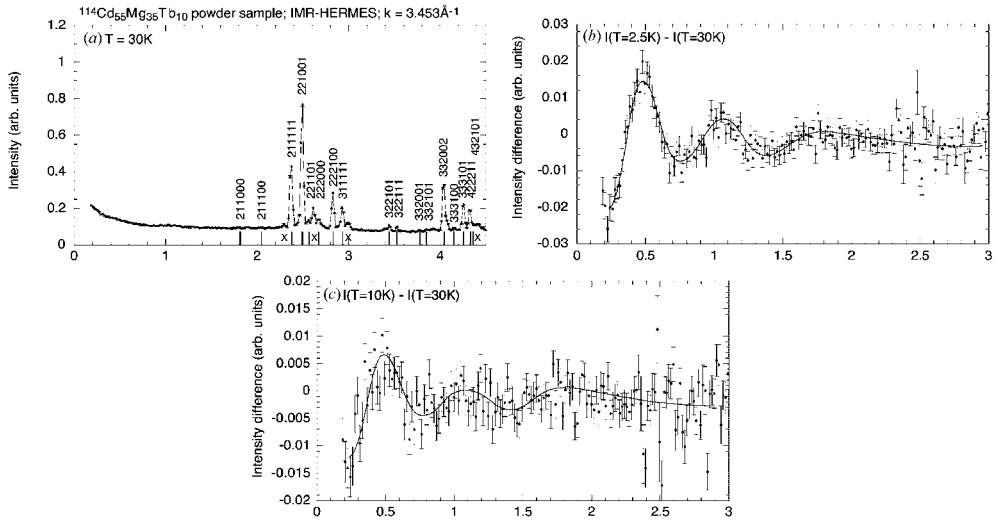


**Figure 8**
(*a*) Neutron diffraction pattern from the single-phased *p*-Cd–Mg–Tb quasicrystal measured at $T = 30$ K. The sample was obtained by annealing the as-cast alloy for 100 h at 723 K. (*b*) Magnetic diffuse scattering pattern at the lowest temperature ($T = 2.5$ K) estimated by the subtraction $I(T = 2.5\ {\rm K}) - I(T = 30\ {\rm K})$. (*c*) Magnetic diffuse scattering pattern at the intermediate temperature ($T = 10$ K) estimated by the subtraction $I(T = 10\ {\rm K}) - I(T = 30\ {\rm K})$. Reprinted from Sato *et al.* (2002). *J. Alloys Compounds*, **342**, 365–368. Copyright (2002), with permission from Elsevier.

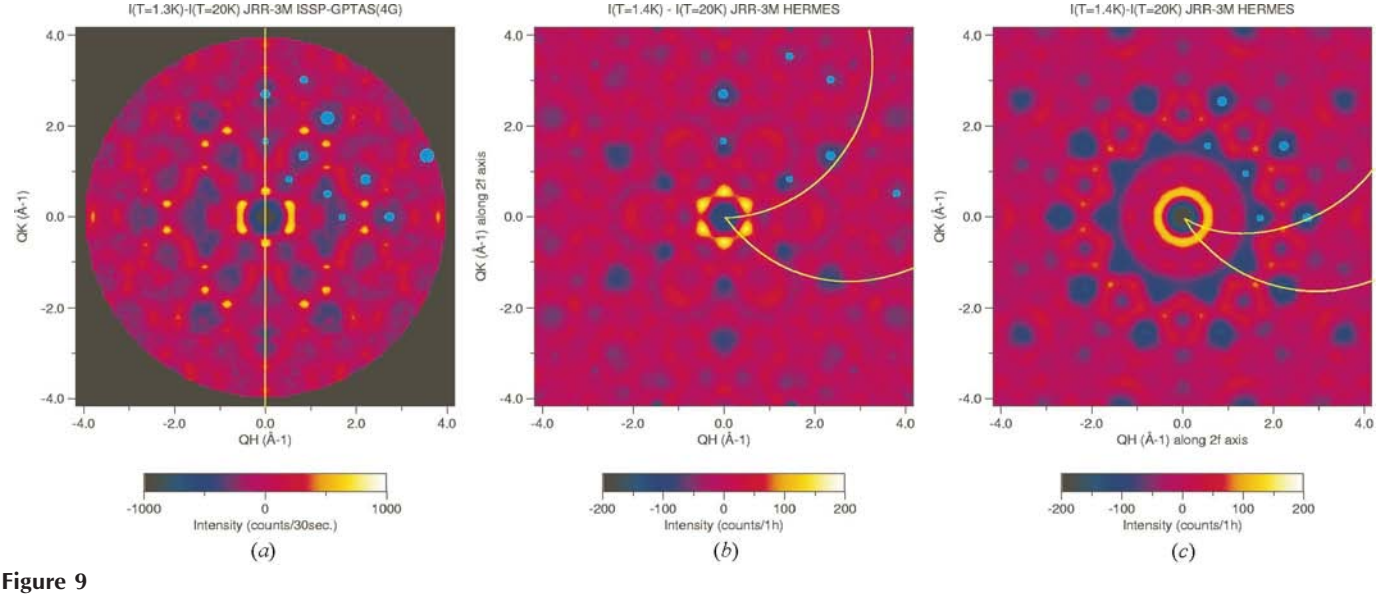


**Figure 9**
Magnetic diffuse scattering maps for the (*a*) 2f, (*b*) 3f and (*c*) 5f planes. The magnetic part was estimated by subtracting higher-temperature ($T = 20$ K) data from the lowest-temperature ($T \simeq 1.3$ K) data. Blue dots in the first quadrant are the positions where the intense nuclear Bragg reflections appear. The regions between the two yellow lines for the 3f and 5f data and the right-half plane for the 2f data are the doubled symmetrically independent regions, where the diffuse scattering was measured. After Sato *et al.* (2000).

dynamics is sufficiently slow, because in the double-axis experiments one observes an energy-integrated scattering function for a certain range (Murani & Heidemann, 1978). The above results clearly show the significant development of the short-range *antiferromagnetic* spin correlations at low temperatures in the *f*-Zn–Mg–*R* quasicrystals. The diffuse scattering develops around the intense nuclear Bragg reflections below $T_{SRC}$, being significantly higher than the macroscopic freezing temperature $T_f$.

### 4.4. Model for the short-range order

There may be at least two different strategies to analyze the diffuse scattering patterns. One is to utilize the 6D crystallography, as is usually done in the atomic structure determination. The analysis method along this line has been developed by Sato *et al.* (2000), to which readers may refer for details. A consequence of this analysis is that the observed diffuse scattering patterns can be interpreted as a 3D projection of virtual diffuse scattering in the 6D reciprocal-lattice space, which is indeed (a square of) a Fourier transform of a 6D short-range spin order with the magnetic modulation vector $\mathbf{q}_m = (\frac{3}{4}, 0, 0, \frac{1}{2}, \frac{3}{4}, \frac{1}{2})$.

The above analysis gives the modulation vector, which is meaningful as a first step to understand the short-range order. However, the next step, which is to determine the spin structure in the real 3D space, seems not a straightforward task in this 6D crystallography approach; firstly, there are too many adjustable parameters for spin directions in the 6D short-range order and, secondly, even if the spin structure could be determined in the 6D space, the spin structure in the real 3D space may not be uniquely projected. Moreover, the short-range nature of the magnetic correlations prevents us from working on the integrated intensity, instead we have to use a

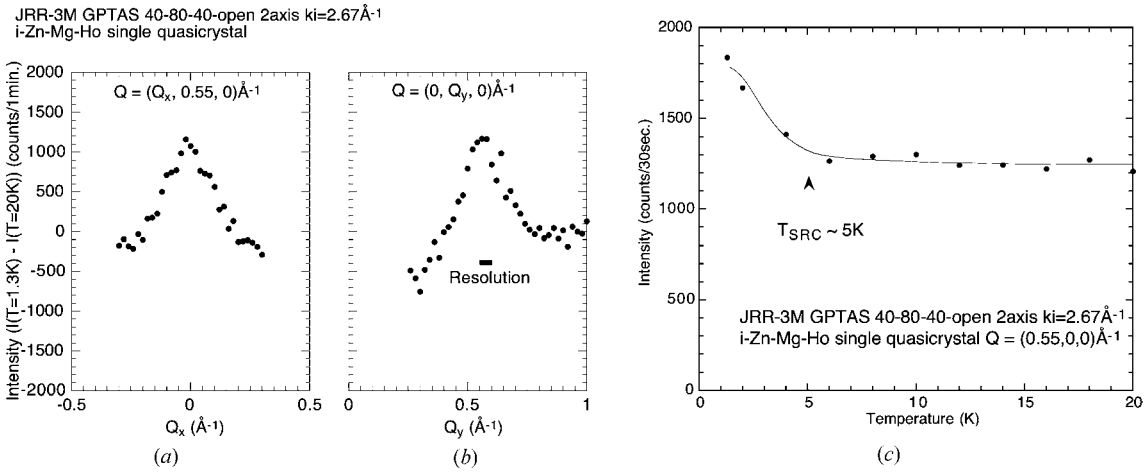


**Figure 10**
Peak profiles of the magnetic diffuse scattering centered at $\mathbf{Q} = (0, 0.55, 0)$ Å$^{-1}$ for (*a*) $Q_x$ and (*b*) $Q_y$ directions. (*c*) Temperature dependence of the diffuse peak intensity observed at $\mathbf{Q} = (0.55, 0, 0)$ Å$^{-1}$. Reprinted figure with permission from Sato *et al.* (2000). *Phys. Rev. B*, **61**, 476–486. Copyright (2000) by the American Physical Society.

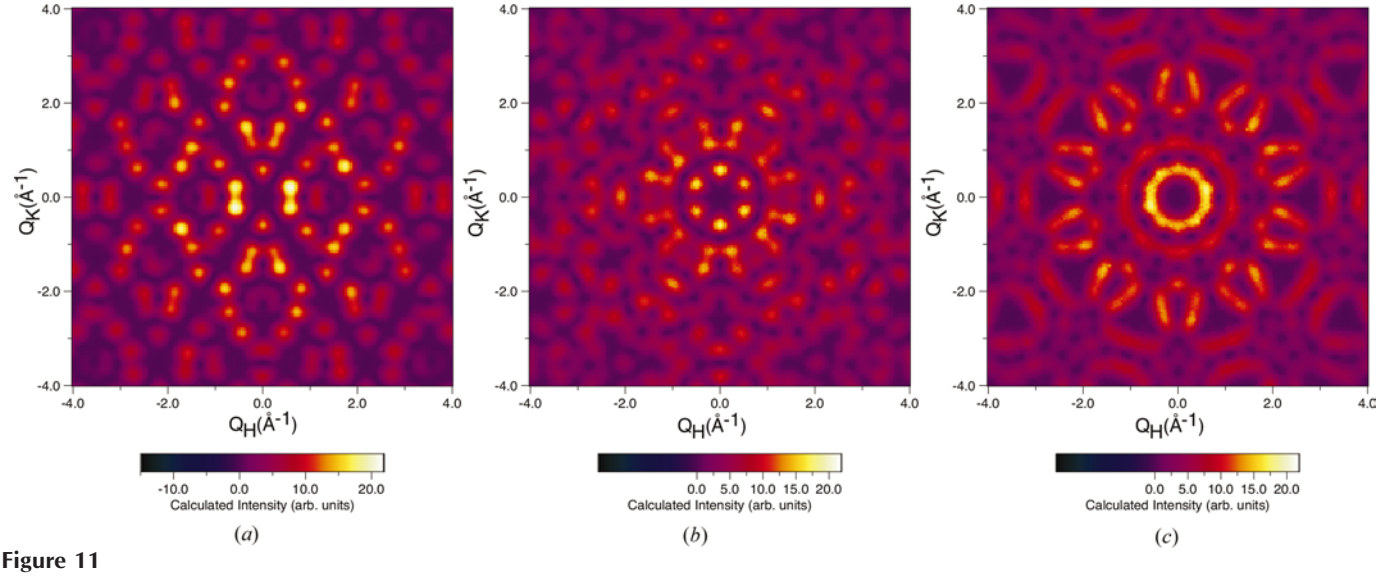


**Figure 11**
Calculated magnetic diffuse scattering maps from the single dodecahedral spin object for the (*a*) 2f, (*b*) 3f and (*c*) 5f planes. The diffuse scattering patterns from the 180 degenerate ground states, obtained from different initial configurations, are statistically averaged.

certain kind of profile fitting method, which further complicates the solving procedure. Thus, we here propose an alternative method to obtain a plausible model for the spin configuration in the short-range-ordered region.

From the magnetic diffuse scattering experiment, we know that the diffuse scattering develops within a small region of the length scale of $\xi \sim 10$ Å. Thus, the first step is to find a rare-earth cluster of comparable size that appears most frequently in the atomic structure model. This is rather a trivial task; as noted in §2, the dominant part of rare-earth sites in the *f*-Zn–Mg–*R* quasicrystals forms a three-dimensional network of edge-sharing dodecahedra. Each dodecahedron has approximate radius $R \sim 7$ Å, which is sufficiently close to $\xi$. Thus, we take this dodecahedral spin cluster as an intrinsic spin object in the *f*-Zn–Mg–*R* quasicrystals. The spins in the adjacent objects may possibly interact with each other, since they indeed share edges; no geometrical reason can be found to neglect the interaction between them. Nevertheless, we here make a conjecture that the observed magnetic diffuse scattering can be explained by the single dodecahedral spin object; this conjecture will be tested in the following.

The dodecahedral spin object has 20 vertices at which the rare-earth spins are situated. For the case of heavy rare-earth elements, the total angular moment ($J$) is quite large, and thus can be approximated by the classical spins. Moreover, both the magnetic susceptibility and neutron inelastic scattering (Sato, Takakura *et al.*, 2001) do not detect significant crystalline-electric field splitting, allowing us to neglect single-site anisotropy as a first approximation. In view of finite electric conductivity in the magnetic quasicrystals, the spin–spin interactions may possibly be given by the Ruderman–Kittel–Kasuya–Yoshida- (RKKY-) type indirect exchange interactions, which only depend on the relative distance of the interacting spins. [It should be noted that the RKKY interaction may not be the same as that in periodic crystals (Roche & Mayou, 1999).] Thus, one may write a model Hamiltonian for the dodecahedral spin object as

$$\mathcal{H} = -\sum_{\langle i,j \rangle} J(R_{ij}) \mathbf{S}_i \cdot \mathbf{S}_j, \tag{2}$$

where $\mathbf{S}_i$ (or $\mathbf{S}_j$) is the Heisenberg classical spin at the $i$th (or $j$th) site and $J(R_{ij})$ is the spin–spin interaction.

Finding a ground state of the above Hamiltonian equation (2) is known to be a non-analytic problem (Axenovich & Luban, 2001). Thus, we use the numerical-minimization technique to find the ground-state spin configuration. For a given set of spin–spin interactions $J$, the ground-state spin configurations are calculated by numerically minimizing equation (2) from a randomly given initial spin structure. It is found that the dodecahedral spin object is highly frustrated for most of the antiferromagnetic $J$'s; there are an infinite number of spin configurations that have the lowest energy, and thus may equally be realized. Thus, we calculate 180 different ground-state spin configurations starting from different initial states and, for each configuration, the diffuse scattering patterns are calculated by the Fourier transform:

$$I(\mathbf{Q}) \propto |f(\mathbf{Q}) \mathbf{S}_\perp(\mathbf{Q})|^2, \tag{3}$$

where $f(\mathbf{Q})$ is the magnetic form factor of the $Ho^{3+}$ ion (Freeman & Desclaux, 1979) and $\mathbf{S}_\perp(\mathbf{Q})$ is defined as

$$\mathbf{S}_\perp(\mathbf{Q}) = \mathbf{S}(\mathbf{Q}) - \frac{\mathbf{Q} \cdot \mathbf{S}(\mathbf{Q})}{Q} \tag{4}$$

and

$$\mathbf{S}(\mathbf{Q}) = \sum_i \exp(-i\mathbf{Q} \cdot \mathbf{R}_i) \mathbf{S}_i. \tag{5}$$

A statistical average is then made for the resulting diffuse scattering patterns and is used as final calculated patterns.

After several trials with different sets of $J$'s, we found that the simplest set of $J$'s that reproduces the observed diffuse scattering patterns is the one comprising only the second-nearest-neighbor interaction $J_2$. The interaction $J_2$ is antiferromagnetic and corresponds to the spin–spin distance of 8.8 Å. The calculated diffuse scattering patterns are shown in Fig. 11; by comparison with the experimental results shown in Fig. 9, one finds quite reasonable agreement. One of the ground-state spin configurations is depicted in Fig. 12. The spins at the opposite side of the dodecahedron have opposite direction (antiferromagnetic), whereas the strong frustration gives rise to the non-collinear spin configurations in the pentagonal faces. The infinite degeneracy allows a continuous change of the spin directions in a certain collective manner without costing energy. The possible relation of this infinite continuous degeneracy to the spin-glass-like behavior will be discussed later.

## 5. Dynamical aspects of spins in quasicrystals

It is undoubtedly crucial to study spin dynamics in magnetic quasicrystals to understand the nature of the spin freezing phenomena. A large number of experiments have been

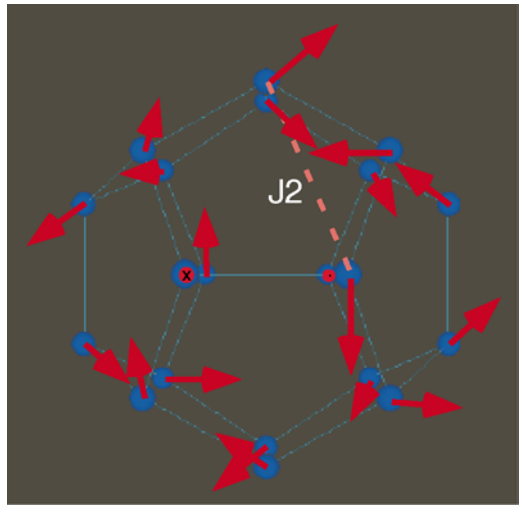


**Figure 12**
One of ground-state spin configurations obtained for the dodecahedral spin object with the antiferromagnetic second-nearest-neighbor interaction $J_2$. It should be noted that the ground state is continuously degenerate, and thus the configuration is not unique.

performed in this direction, with a wide range of observation time scales.

The slowest experiment may be the ac susceptibility and magnetization-relaxation measurements. Experiments falling into this category were performed by Charrier & Schmitt (1998), Fisher *et al.* (1999) and Dolinšek *et al.* (2001, 2003). The former two experiments reported that time relaxation of the magnetization in the *f*-Zn–Mg–*R* quasicrystals is given by the stretched exponential function, as commonly seen in the canonical spin-glasses (Mydosh, 1993). Fisher *et al.* (1999) also detected the divergence of the real part of the third-order ac susceptibility $\chi_3$. From those experimental results, Fisher *et al.* (1999) concluded that the spin freezing in the *f*-Zn–Mg–*R* quasicrystals is the thermodynamic spin-glass transition. On the other hand, in the later experiments by Dolinšek *et al.* (2001, 2003), detailed information on the decay of the thermoremanent magnetization (TRM) was obtained in a low-magnetic-field region with temperatures slightly lower than $T_f$ in the *f*-Zn–Mg–*R* and *p*-Cd–Mg–*R* quasicrystals. They found that the amplitude of TRM shows linearly increasing dependence on the external field. This is apparently incompatible with the canonical spin-glasses, where an ultrametrically organized free-energy landscape is believed to be manifested below $T_f$. The linear increase rather indicates a single global free-energy minimum, and thus is indicative of the superparamagnetic origin of the spin freezing; here the freezing behavior can be interpreted as blocking of spins in finite-sized non-interacting clusters. It is also noted that this spin freezing is similar to the one observed in geometrically frustrated magnets, such as antiferromagnetically interacting spins on the Kagome or pylochlore lattice (Gaulin *et al.*, 1992; Schiffer *et al.*, 1995; Gingras *et al.*, 1997; Wills *et al.*, 2000).

A probe measuring relatively fast spin dynamics may be the μSR technique (Noakes *et al.*, 1998; Charrier *et al.*, 1999). In the μSR signal, the dominant part of the relaxations is the stretched-exponential type, being consistent with the spatially random freezing of the spins. The μSR experiments, in addition, detect the other components of unknown origin; Noakes *et al.* (1998) reported coexisting temperature-independent relaxation, whereas Charrier & Schmitt found a simple exponential term. These additional signals may be intriguing for further study. Spin dynamics with the fastest time scales, *i.e.* $10^{-12}$ s can be observed by the neutron inelastic scattering technique. Preliminary results have been reported in the literature (Sato *et al.*, 1999; Scheffer *et al.*, 2000; Sato, Takakura *et al.*, 2001), however, the details of the spin dynamics in this time range have not been elucidated completely.

## 6. Are magnetic quasicrystals spin-glasses?

After intensive study of more than a decade, it now becomes possible to draw conclusions on the spin ordering in the rare-earth-based magnetic quasicrystals. Firstly, as confirmed by several neutron diffraction experiments, the magnetic order is short-ranged; magnetic correlations develop as temperature is decreased, nevertheless, the development terminates with finite correlation lengths. The 3D analysis of the magnetic diffuse scattering at the lowest temperature shows that the dodecahedral spin object is intrinsic for the short-range order.

A coherent picture is also inferred from the TRM measurements. They also indicate that the free-energy landscape is not ultrametrically organized in the magnetic quasicrystals but has one global minimum as is the case for the superparamagnets. This is, indeed, in agreement with the above-described neutron diffraction results, where existence of rather rigid spin objects is evidenced. It should be noted that the dodecahedral spin object with Heisenberg isotropic spins cannot have a free-energy minimum since the ground state becomes isotropic and thus flipping of entire spins does not cost energy. However, in reality, there must be a weak but non-negligible anisotropy due to the non-spherical site symmetry. This perturbation term, which we neglected in the model Hamiltonian for simplicity, will break the Heisenberg isotropy, as well as continuous degeneracy of the ground state. This may result in an energy barrier for the flipping of entire cluster spins. Therefore we may conclude that the spin freezing phenomenon, observed in the magnetic quasicrystal, is related to that of the superparamagnet; the intrinsic spin object for the blocking phenomenon may most likely be the rare-earth dodecahedron.

Although we now have a relatively simple interpretation for the freezing phenomenon in magnetic quasicrystals, there remains one fundamental question: why does the development of the spin correlations terminate at finite lengths? As noted before, there is no geometrical reason that disconnects each dodecahedral object from the adjacent ones. Nevertheless, the fact that the observed diffuse scattering can be explained by the single object strongly suggests that there is some sort of mechanism that prohibits the development of the correlation out of the dodecahedral spin object. For this puzzle, it may be suggestive that waves in a quasiperiodic structure, such as phonons or electrons, are likely to have a localization tendency (Rieth & Schreiber, 1998; Fujiwara, 1999; Hafner & Krajčí, 1999). The spin fluctuations in the paramagnetic phase are also a collective motion of spins in short-range regions, and thus the same localization mechanism may work for the spin fluctuations.

For the *p*-Cd–Mg–*R* and *p*-Zn–Mg–*R* quasicrystals, the details of the spin freezing are not elucidated yet. We think that they are very intriguing; the *p*-Cd–Mg–*R* quasicrystals show two successive anomalies of unknown origin, whereas the *p*-Zn–Mg–*R* quasicrystals are of interest due to their primitive icosahedral lattice. It is thus highly desirable to perform single-quasicrystal neutron diffraction on these systems.

Another future issue is to find a magnetic quasicrystal that exhibits long-range spin order. It is trivial that ferromagnetic order is realized if the spin–spin interactions are dominantly ferromagnetic, even in the quasiperiodic lattice. On the other hand, for antiferromagnetic interactions, long-range order may be expected if the network of spins has no geometrical frustrations. It is thus always desired to find new quasicrystalline materials with different structures. From this viewpoint, the recently discovered Zn–Fe–Sc quasicrystal may be very

interesting (Maezawa *et al.*, 2004), since the magnetic Fe sites are expected to have quasiperiodic structure different to the *A*–Mg–*R* quasicrystals.

## 7. Conclusions

In this review, we have summarized recent experimental activity on spin freezing phenomena in the *A*–Mg–*R* (*A* = Cd, Zn; *R* = rare-earth elements) magnetic quasicrystals. The macroscopic magnetization measurements and the microscopic neutron diffraction now give a coherent picture for the freezing phenomena at least for the *f*-Zn–Mg–*R* quasicrystals; the freezing may be interpreted as blocking of the total spin of the dodecahedral spin object. There is a remaining fundamental question: why can the dodecahedral spin objects be treated separately even though the spin objects should interact with each other?

The present author would like to express his sincere thanks to all collaborators, Drs A. P. Tsai, H. Takakura, K. Shibata, K. Ohoyama, K. H. Andersen, H. Kadowaki, J. Dolinsek, J. W. Lynn and S. H. Lee, for their continuous support. He also thanks Drs I. R. Fisher, Z. Islam and B. Charrier for stimulating discussions, and many others for various contributions.

## References


Abe, E., Takakura, H. & Tsai, A. P. (2001). *J. Electron Microsc.* **50**, 187–195.

Achiam, Y., Lubensky, T. C. & Marshall, E. W. (1986). *Phys. Rev. B*, **33**, 6460–6464.

Aoyama, H. & Odagaki, T. (1987). *J. Stat. Phys.* **48**, 503–511.

Axenovich, M. & Luban, M. (2001). *Phys. Rev. B*, **63**, 100407-1–4.

Bahadur, D. (1997). *Prog. Cryst. Growth Charact.* **34**, 287–301.

Ball, M. D. & Lloyd, D. J. (1985). *Scr. Metall.* **19**, 1065–1068.

Binder, K. & Young, A. P. (1986). *Rev. Mod. Phys.* **58**, 801–976.

Boudard, M. & de Boissieu, M. (1999). *Physical Properties of Quasicrystals*, edited by Z. M. Stadnik, pp. 91–126. Berlin: Springer-Verlag.

Brühne, S., Sterzel, R., Uhrig, E., Gross, C. & Assmus, W. (2003). *Medium Range Real Atomic Structure of Face Centered Icosahedral* $Ho_9Mg_{26}Zn_{65}$. Cond-Mater/0302416.

Brühne, S., Uhrig, E., Gross, C. & Assmus, W. (2004). *Cryst. Res. Technol.* **38**, 1023–1036.

Cervellino, A., Haibach, T. & Steurer, W. (2002). *Acta Cryst*, B**58**, 8–33.

Charrier, B., Cotrell, S. & Schmitt, D. (1999). *Physica B*, **266**, 165–172.

Charrier, B., Hazemann, J. L. & Schmitt, D. (1998). *J. Alloys Compounds*, **281**, 117–122.

Charrier, B., Ouladdiaf, B. & Schmitt, D. (1997). *Phys. Rev. Lett.* **78**, 4637–4640.

Charrier, B. & Schmitt, D. (1997). *J. Magn. Magn. Mater.* **171**, 106–112.

Charrier, B. & Schmitt, D. (1998). *J. Magn. Magn. Mater.* **189**, 165–172.

Chernikov, M. A., Bernasconi, A., Beeli, C., Schilling, A. & Ott, H. R. (1993). *Phys. Rev. B*, **48**, 3058–3065.

Dolinšek, J., Jagličić, Z., Chernikov, M. A., Fisher, I. R. & Canfield, P. C. (2001). *Phys. Rev. B*, **64**, 224209-1–4.

Dolinšek, J., Jagličić, Z., Sato, T. J., Guo, J. Q. & Tsai, A. P. (2003). *J. Phys. Condens. Matter*, **15**, 7981–7996.

Fisher, I. R., Cheon, K. O., Panchula, A. F., Canfield, P. C., Chernikov, M., Ott, H. R. & Dennis, K. (1999). *Phys. Rev. B*, **59**, 308–321.

Freeman, A. J. & Desclaux, J. P. (1979). *J. Magn. Magn. Mater.* **12**, 11–21.

Fujiwara, T. (1989). *Phys. Rev. B*, **40**, 942–946.

Fujiwara, T. (1999). *Physical Properties of Quasicrystals*, edited by Z. M. Stadnik, pp. 169–207. Berlin: Springer-Verlag.

Fujiwara, T. & Yokokawa, T. (1991). *Phys. Rev. Lett.* **66**, 333–336.

Fukamichi, K. (1999). *Physical Properties of Quasicrystals*, edited by Z. M. Stadnik, pp. 295–326. Berlin: Springer-Verlag.

Gaulin, B. D., Reimers, J. N., Mason, T. E., Greedan, J. E. & Tun, Z. (1992). *Phys. Rev. Lett.* **69**, 3244–3247.

Gingras, M. J. P., Stager, C. V., Raju, N. P., Gaulin, B. D. & Greedan, J. E. (1997). *Phys. Rev. Lett.* **78**, 947–950.

Godrèche, C., Luck, J. M. & Orland, H. (1986). *J. Stat. Phys.* **45**, 777–800.

Guo, J. Q., Abe, E. & Tsai, A. P. (2000). *Jpn. J. Appl. Phys. Part 2*, **39**, L770–L771.

Hafner, J. & Krajčí, M. (1999). *Physical Properties of Quasicrystals*, edited by Z. M. Stadnik, pp. 209–256. Berlin: Springer-Verlag.

Hattori, Y., Fukamichi, K., Suzuki, K., Niikura, A., Tsai, A. P., Inoue, A. & Masumoto, T. (1995). *J. Phys. Condens. Matter*, **7**, 4183–4191.

Hattori, Y., Niikura, A., Tsai, A. P., Inoue, A., Masumoto, T., Fukamichi, K., Aruga-Katori, H. & Goto, T. (1995). *J. Phys. Condens. Matter*, **7**, 2313–2320.

Hiramoto, H. & Kohmoto, M. (1989). *Phys. Rev. B*, **40**, 8225–8234.

Ishimasa, T., Oyamada, K., Arichika, Y., Nishibori, E., Takata, M., Sakata, M. & Kato, K. (2003). *J. Non-Cryst. Solids*, **334**, 167–172.

Islam, Z., Fisher, I. R., Zarestky, J., Canfield, P. C., Stassis, C. & Goldman, A. I. (1998). *Phys. Rev. B*, **57**, R11047–R11050.

Kashimoto, S., Matsuo, S., Nakano, H., Shimizu, T. & Ishimasa, T. (1999). *Solid State Commun.* **109**, 63–67.

Kohmoto, M., Sutherland, B. & Tang, C. (1987). *Phys. Rev. B*, **35**, 1020–1033.

Ledue, D., Teillet, J., Carnet, J. & Dujardin, J. (1993). *J. Non-Cryst. Solids*, **153&154**, 403–407.

Lifshitz, R. (1998). *Phys. Rev. Lett.* **80**, 2717–2720.

Luo, Z., Zhang, S., Tang, Y. & Zhao, D. (1993). *Scr. Metal. Mater.* **28**, 1513–1518.

Maezawa, R., Kashimoto, S. & Ishimasa, T. (2004). *Philos. Mag. Lett.* **84**, 215–223.

Matsuo, S., Nakano, H., Ishimasa, T. & Mori, M. (1993). *J. Phys. Soc. Jpn.* **62**, 4044–4052.

Murani, A. P. & Heidemann, A. (1978). *Phys. Rev. Lett.* **41**, 1402–1406.

Mydosh, J. A. (1993). *Spin Glasses: an Experimental Introduction.* London: Taylor and Francis.

Niikura, A., Tsai, A. P., Inoue, A. & Masumoto, T. (1994). *Philos. Mag. Lett.* **69**, 351–355.

Noakes, D. R., Kalvius, G. M., Wäppling, R., Stronach, C. E., White, M. F. Jr, Saito, H. & Fukamichi, K. (1998). *Phys. Lett. A*, **283**, 197–202.

Ohashi, W. & Spaepen, F. (1987). *Nature (London)*, **330**, 555–556.

Okabe, Y. & Niizeki, K. (1990). *Quasicrystals*, edited by T. Fujiwara & T. Ogawa, pp. 206–214. Berlin: Springer-Verlag.

Rau, D., Gavilano, J. L., Mushkolaj, S., Beeli, C., Chernikov, M. A. & Ott, H. R. (2003). *Phys. Rev. B*, **68**, 134204-1–8.

Reid, R. W., Bose, S. K. & Mitrović, B. (1998). *J. Phys. Condens. Matter*, **10**, 2303–2321.

Rieth, T. & Schreiber, M. (1998). *J. Phys. Condens. Matter*, **10**, 783–800.

Roche, S. & Mayou, D. (1999). *Phys. Rev. B*, **60**, 322–328.

Sato, T. J., Guo, J. Q. & Tsai, A. P. (2001). *J. Phys. Condens. Matter*, **13**, L105–L111.

Sato, T. J., Takakura, H., Guo, J. Q., Tsai, A. P. & Ohoyama, K. (2002). *J. Alloys Compounds*, **342**, 365–368.

Sato, T. J., Takakura, H. & Tsai, A. P. (1998). *Jpn. J. Appl. Phys.* **37**, L663–L665.
Sato, T. J., Takakura, H., Tsai, A. P., Kadowaki, H. & Shibata, K. (2001). *J. Phys. Soc. Jpn. Suppl.* **70**, 224–226.
Sato, T. J., Takakura, H., Tsai, A. P. & Shibata, K. (1998). *Phys. Rev. Lett.* **81**, 2364–2367.
Sato, T. J., Takakura, H., Tsai, A. P., Shibata, K., Ohoyama, K. & Andersen, K. H. (1999). *Magnetic Correlations in the Zn-Mg-RE Icosahedral Quasicrystals*. Presented at the 7th International Conference on Quasicrystals, Stuttgart, Germany.
Sato, T. J., Takakura, H., Tsai, A. P., Shibata, K., Ohoyama, K. & Andersen, K. H. (2000). *Phys. Rev. B*, **61**, 476–486.
Scheffer, M., Rouijaa, M., Suck, J. B., Sterzel, R. & Lechner, R. E. (2000). *Mater. Sci. Eng.* A**294–296**, 488–491.
Schiffer, P., Ramirez, A. P., Huse, D. A., Gammel, P. L., Yaron, U., Bishop, D. J. & Valentino, A. J. (1995). *Phys. Rev. Lett.* **74**, 2379–2382.
Sebastian, S. E., Huie, T., Fisher, I. R., Dennis, K. W. & Kramer, M. J. (2004). *Philos. Mag.* **84**, 1029–1037.
Shechtman, D., Blech, I., Gratias, D. & Cahn, J. W. (1984). *Phys. Rev. Lett.* **53**, 1951–1953.
Sterzel, R., Gross, C., Kounis, A., Miehe, G., Fuess, H., Reutzel, S., Holland-Moritz, D. & Assmus, W. (2002). *Philos. Mag. Lett.* **82**, 443–450.
Steurer, W. & Haibach, T. (1999). *Physical Properties of Quasicrystals*, edited by Z. M. Stadnik, pp. 51–89. Berlin: Springer-Verlag.
Takakura, H., Shiono, M., Sato, T. J., Yamamoto, A. & Tsai, A. P. (2001). *Phys. Rev. Lett.* **86**, 236–239.
Tsai, A. P. (1999). *Physical Properties of Quasicrystals*, edited by Z. M. Stadnik, pp. 5–50. Berlin: Springer-Verlag.
Tsai, A. P., Guo, J. Q., Abe, E., Takakura, H. & Sato, T. J. (2000). *Nature (London)*, **408**, 537–538.
Tsai, A. P., Inoue, A. & Masumoto, T. (1987). *Jpn. J. Appl. Phys.* **26**, L1505–L1507.
Tsai, A. P., Niikura, A., Inoue, A., Masumoto, T., Nishida, Y., Tsuda, K. & Tanaka, M. (1994). *Philos. Mag. Lett.* **70**, 169–170.
Tsai, A. P., Sato, T. J., Guo, J. Q. & Hirano, T. (1999). *J. Non-Cryst. Solids*, **250–252**, 833–838.
Tsunetsugu, H., Fujiwara, T., Ueda, K. & Tokihiro, T. (1986). *J. Phys. Soc. Jpn*, **55**, 1420–1423.
Tsunetsugu, H., Fujiwara, T., Ueda, K. & Tokihiro, T. (1991). *Phys. Rev. B*, **43**, 8879–8891.
Tsunetsugu, H. & Ueda, K. (1987). *Phys. Rev. B*, **36**, 5493–5499.
Wills, A. S., Dupuis, V., Vincent, E., Hammann, J. & Calemczuk, R. (2000). *Phys. Rev. B*, **62**, R9264–R9267.
Yamamoto, A. (1996). *Acta Cryst.* A**52**, 509–560.
Yamamoto, A., Takakura, H. & Tsai, A. P. (2003). *Phys. Rev. B*, **68**, 094201-1–3.